JACS
JOURNAL OF THE AMERICAN CHEMICAL SOCIETY
pubs.acs.org/JACS
Article

Surprising Rigidity of Functionally Important Water Molecules Buried in the Lipid Headgroup Region

Rongfu Zhang, Timothy A. Cross,* Xinhua Peng, and Riqiang Fu*

Cite This: J. Am. Chem. Soc. 2022, 144, 7881−7888
Read Online

ABSTRACT: Understanding water dynamics and structure is an important topic in biological systems. It is generally held in the literature that the interfacial water of hydrated phospholipids is highly mobile, in fast exchange with the bulk water ranging from the nano- to femtosecond timescale. Although nuclear magnetic resonance (NMR) is a powerful tool for structural and dynamic studies, direct probing of interfacial water in hydrated phospholipids is formidably challenging due to the extreme population difference between bulk and interfacial water. We developed a novel ^{17}O solid-state NMR technique in combination with an ultra-high-field magnet (35.2 T) to directly probe the functionally important interfacial water. By selectively suppressing the dominant bulk water signal, we observed two distinct water species in the headgroup region of hydrated dimyristoylphosphatidylcholine (DMPC) lipid bilayers for the first time. One water species denoted as "confined water" is chemically and dynamically different from the bulk water (~0.17 ppm downfield and a slightly shorter spin-lattice relaxation time). Another water species denoted as "bound water" has severely restricted motion and a distinct chemical shift (~12 ppm upfield). Additionally, the bulk water is not as "free" as pure water, resulting from the fast exchange with the water molecules that weakly and transiently interact with the lipid choline groups. These new discoveries clearly indicate the existence of the interfacial water molecules that are relatively stable over the NMR timescale (on the order of milliseconds), providing an opportunity to characterize water dynamics on the millisecond or slower timescale in biomacromolecules.

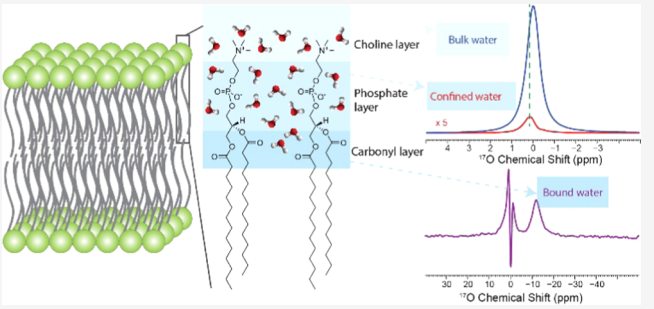

1. INTRODUCTION

Water is ubiquitous yet essential for the existence of known life forms.[1] It is crucial, both structurally and functionally for biomolecules, including proteins, nucleic acids, and membranes.[2,3] Studies of water structure and dynamics are fundamentally important for understanding biological systems. One example involves the study of interfacial water in biological membranes, which is a complex organization of lipids, water, and proteins. These membranes are critical for life by compartmentalizing organelles and hosting proteins that permit selective molecules and ions to passage into and out of cells.[2] When exposed to water, lipids self-assemble into bilayers composed of the hydrophilic lipid headgroups solvated into the bulk aqueous environment and the hydrocarbon fatty acyl chains forming the hydrophobic core of cellular membranes through which water permeation is greatly restricted.[2] Figure 1 schematically illustrates the lipid bilayer structure using hydrated dimyristoylphosphatidylcholine (DMPC) lipids as a model. In the hydrophilic surface of the bilayer, the interfacial water layers have an approximate thickness of ~1 nm between the fatty acyl chains and the choline nitrogen, with the first water layer in the vicinity of the glycerol C3 ester linkage that has the slowest exchange rate.[4] The hydration shells in the headgroup region can be graded by the stability of the water molecules. The deeper into the lipid headgroup region, the greater the reduction in water and headgroup dynamics and hence increased stability of the water molecules. The mixed charge and polarity (e.g., positively charged choline group and negatively charged phosphate group) in the headgroup affect the local hydrogen-bonding network.

Many technologies as well as molecular dynamics (MD) approaches have been applied to hydrated lipid bilayers for the purpose of characterizing the water interactions and the timescale for water exchange with bulk water.[5,6] These experimental technologies, including heterodyne-detected vibrational sum-frequency generation (HD-VSFG) spectroscopy,[7] quasi-elastic neutron scattering (QENS),[8] terahertz time-domain spectroscopy (TTDS),[9] small-angle X-ray scattering spectroscopy (SAXS)[10] and small angle neutron scattering spectroscopy (SANS),[11] Fourier-transform infrared spectroscopy (FTIR),[12,13] and MD calculations,[14−16] are primarily restricted to timescales that are sub-nanosecond. Despite being

Received: February 24, 2022
Published: April 19, 2022

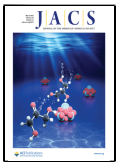

https://doi.org/10.1021/jacs.2c02145
J. Am. Chem. Soc. 2022, 144, 7881−7888

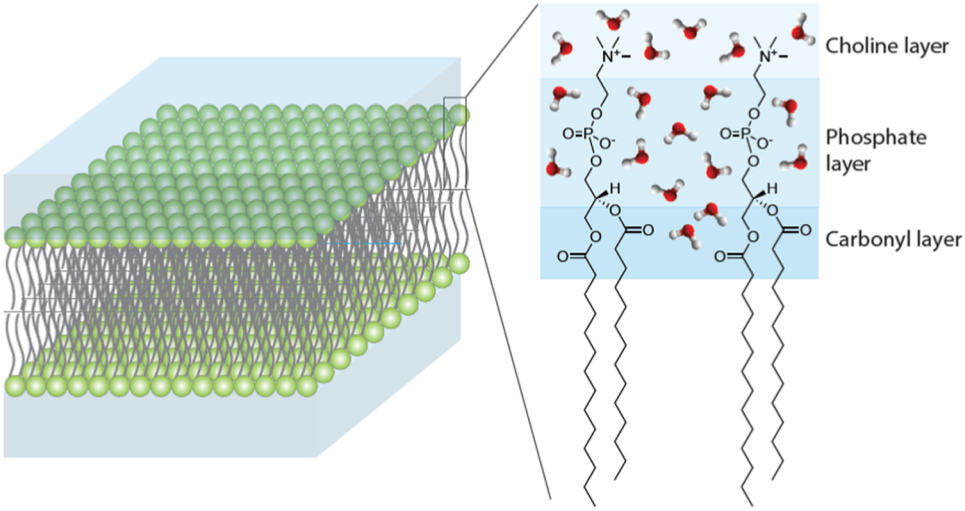

Figure 1. Schematic model of the hydrated DMPC bilayer. The hydration of the headgroup region is highlighted with different blue background shading, reflecting the waters that interact with the choline, phosphate, and carbonyl groups of the lipid headgroups.

restricted to these short timescales, it has been determined from HD-VSFG[7] that the choline groups accept weaker hydrogen bonds from water while phosphate groups accept stronger water hydrogen bonds. QENS[8] and TTDS[9] found that there were rigid waters on the nano- to picosecond timescale, while SAXS and SANS[10,11] identified 7−8 waters in the headgroup region per lipid. FTIR[12,13] identified multiple water binding sites through the changes in the bond vibration frequency due to hydrogen bonding with water. MD[14−16] results are dependent on the water model, such that different dipole potentials were calculated when TIP3P and TIP4P were used and may underestimate the stability of the waters by orders of magnitude as was done for the waters in the aqueous pore of gramicidin A (gA).[17] Nuclear magnetic resonance (NMR) is capable of studying molecular dynamics over a wide timescale, ranging from picoseconds to seconds. Deuterium NMR has been used to study the water dynamics in the lipid bilayers using deuterated water.[18,19] Generally, the observed ^{2}H NMR spectra of water exhibited a much smaller quadrupolar coupling (a few kHz) than that (∼220 kHz) of the rigid water, indicating that the majority of the water molecules in the lipid environments are highly mobile. When considering the fast exchange between two types of water molecules, i.e., the trapped water with no quadrupolar coupling as in the free water and "bound" water (with a small residual quadrupolar coupling), about 10 "bound" water molecules per lipid could be characterized through the dependence of the observed ^{2}H quadrupolar splitting as a function of DMPC-to-D_2O molar ratio.[19] However, even under their relatively high DMPC-to-D_2O molar ratio, those so-called "bound" water molecules were still highly mobile, as their quadrupolar splitting was small.

Such short-lived water states[20−22] make it difficult to understand the important biological function and structural aspects associated with these waters that have been reported extensively.[23−26] It has not been recognized until recently that water's mobility in constrained biological systems can be a lot slower than what had been anticipated (nano- to picosecond timescale).[17,27] For example, the water exchange rate between different bound water sites in the gA pore had been thought to be on the sub-nanosecond timescale; however, recent results based on ^{17}O spectroscopy of the gA carbonyl oxygens found it to be on the millisecond timescale when an ion gradient across the membrane was not present—a difference of 6 orders of magnitude.[17] Since much of what is known about the waters in the phospholipid headgroup environment is known from MD simulations and fast-timescale experimental methods, the unique capability of NMR technology to characterize slow dynamics (milli- to nanosecond) allows for the opportunity to identify additional water species on a slower timescale that may have important biological significance.

^{17}O is a nucleus whose quadrupolar coupling is sensitive to dynamics, while its chemical shift is very sensitive to the chemical environment. It is thus appealing to study water dynamics and interactions directly using ^{17}O NMR spectroscopy. However, several difficulties hinder the routine application of ^{17}O NMR as a research tool: the low natural abundance (∼0.037%); the low gyromagnetic ratio (∼1/7th of ^{1}H isotope); the intrinsic quadrupolar spin property; and the low population of potential bound water molecules associated with lipid bilayers.

To overcome these difficulties, we utilized the ultra-high-field (35.2 T or 1.5 GHz for ^{1}H) of the series-connected-hybrid (SCH) magnet at the National High Magnetic Field Laboratory[28,29] and ^{17}O-enriched water, which dramatically improves both resolution and sensitivity for ^{17}O spectra. This allows for the direct detection of water molecules having lifetimes on the millisecond timescale, a very different timescale than the previous water studies. However, there is still a fundamental problem before such bound waters can be detected and that is that typical lipid bilayer preparations may have orders of magnitude more bulk water than bound water.[30,31] Such a bound water signal would be completely buried under the bulk water signals and consequently become indistinguishable from the bulk water. It is therefore virtually impossible to directly observe the ^{17}O NMR signal of bound water without substantial suppression of the bulk water.

Here, we first introduce a novel selective ^{17}O solid-state NMR technique to significantly suppress the bulk water signal while maintaining the signal of bound water for direct detection. With this new method, we identified a small portion of less-mobile water molecules whose chemical shift and dynamics are distinctly different from the bulk water. Notably, we have observed a class of bound water that preserves a large

https://doi.org/10.1021/jacs.2c02145
J. Am. Chem. Soc. 2022, 144, 7881−7888

quadrupolar coupling. These observations provide us with a new picture of how water interacts with specific sites in the cell membrane interface on a long timescale.

2. MATERIALS AND METHODS

2.1. Preparation of MAS and Oriented Samples. *2.1.1. MAS Sample Preparation.* Briefly, 30 mg of powdered dimyristoylphosphatidylcholine (DMPC) lipids (Avanti Polar Lipids) was dissolved in 2 mL of trifluoroethanol/benzene (J.T. Baker and Sigma) solvent (v/v = 1/1). Upon flash-freezing in liquid nitrogen, the sample was placed in a vacuum chamber for 24 h to obtain a fluffy DMPC lipid powder. Then, 30 μL of 5 mM Tris-HCl (pH 7.5) in 80% ^{17}O-enriched water was added directly to the DMPC lipid powder, and the sample tube was quickly sealed to avoid any water loss or dilution of the ^{17}O label. The sample was then allowed to equilibrate at 37° C in an incubation oven for at least 2 days until a translucent DMPC liposome sample was formed. Low *g*-force (2000*g*) centrifugation was used to collect the prepared sample. The hydrated DMPC liposomes with 80% ^{17}O labeled water were then packed into a 3.2 mm pencil rotor with a homemade packing tool. The final hydrated DMPC liposome had a water content of ∼50%.

2.1.2. Aligned Sample Preparation. Typically, 20 mg of powdered DMPC lipids (Avanti Polar Lipids) was solubilized in 0.4 mL of trifluorethanol/benzene (J.T. Baker and Sigma) solvent (v/v = 1/1). The solution was then deposited on ∼40 glass slides (Matsunami, Osaka, Japan). The solvent was evaporated in a chemical hood and then thoroughly dried overnight in a vacuum chamber. Then, 0.5 μL of 5 mM Tris-Cl (pH 7.5) in 80% ^{17}O-enriched water was added directly to each slide and immediately stacked. The stacked glass slides were inserted into a glass sample cell and sealed with wax to avoid loss of water. The sealed sample was then allowed to equilibrate in a 37 °C incubation oven for at least 1 week. The final aligned DMPC bilayers have a water content of ∼50%.

2.2. Selective ^{17}O Solid-State NMR Spectroscopy. As highlighted in green in Figure 2A, the multiple pulses having the same pulse length but different phases are applied one after another. As detailed in the Supporting Information, such a train of pulses scales the magnetization along the *z*-axis (parallel to the magnetic field) according to their respective pulse flip angle, θ, before being brought to the *xy* plane for detection by the last $(n + 1)$th pulse

$$S_Z = [1-\cos(2)]^n \epsilon_n \quad (1)$$

Here, S_Z represents the scaling factor and ϵ_n is derived to be 1, 1/2, 1/4, and 1/8 for n = 0, 1, 2, and 3, respectively. The individual phase for each pulse is designed using the rotation tree diagram, as shown in Figure S1. For the half-integer ^{17}O nucleus (spin-5/2), the nutation frequency is ν_1 for all transitions when $\nu_1/\nu_q \gg 1$, but it becomes $3\nu_1$ for the central transition when $\nu_1/\nu_q \ll 1$. Here, ν_1 and ν_q represent the applied radio-frequency (RF) amplitude and quadrupolar coupling constant.[32,33] Therefore, the multiple pulses highlighted in Figure 2A can be used to differentiate ^{17}O signals by the size of their quadrupolar couplings, as discussed in detail in the Supporting Information.

2.3. Experimental Section. ^{17}O oriented and MAS NMR measurements were performed at 1.5 GHz on the SCH magnet using a Bruker NEO console, where the ^{17}O Larmor frequency is 203.36 MHz. Similar MAS NMR measurements were also conducted on an 800 MHz NMR spectrometer equipped with a Bruker NEO console, where the ^{17}O Larmor frequency is 108.44 MHz. The sample spinning rate was controlled by a Bruker pneumatic MAS unit at 12 kHz ± 3 Hz, and the sample temperature was maintained well above the phase-transition temperature of DMPC lipid (∼22 °C) for all NMR measurements. The ^{17}O 90° pulse length was calibrated to be 6.0 μs using bulk water from the sample, which was also used as a reference at 0 ppm. The inversion recovery spin-lattice relaxation time (T_1) measurements for bulk water utilized a 180°-pulse (i.e., 12 μs) that was applied, followed by the recovery time τ_d, while θ was set to 6 μs (i.e., 90° pulse) and τ_m = 0 for detection. Briefly, 64 scans were used for the T_1 measurements. When the 180°-pulse (i.e., 12 μs) was applied, followed by a fixed τ_d of 2.6 ms (according to the measured T_1 value), the bulk water signal crossed the *xy* plane (the so-called zero-crossing) so that it was minimized for detection. Under these settings, when θ was set to 6 μs (i.e., 90° pulse), varying τ_m permitted the T_1 measurement of the confined water species. On the other hand, when τ_m = 0 and θ was set to 1.5 μs (i.e., corresponding to a 22.5° flip angle for bulk water and 67.5° flip angle for the bound water having a large quadrupolar coupling), the bulk water signal could be selectively suppressed substantially, allowing for the observation of the bound water signal. In this experiment, 92,160 scans were used to accumulate the signals with a recycle delay of 50 ms. For the experiments at 800 MHz, 409,600 scans were obtained for signal accumulations. For the aligned sample, θ was set to 4.0 μs (corresponding to a 60° flip angle) and 8836 scans were used to accumulate the signals with a recycle delay of 50 ms.

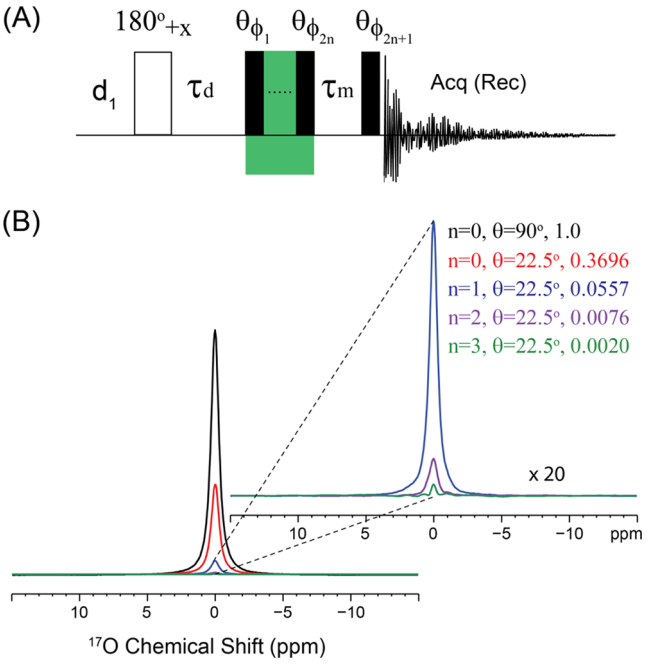

Figure 2. (A) Pulse sequence used in the experiments. The phase cycling designs for the pulses with flip angle θ are detailed in Figure S1. The 180°-pulse at the beginning is used for the inversion recovery spin-lattice relaxation measurements. (B) Experimentally observed bulk water signals (without the 180°-pulse) under different experimental conditions. The experimental conditions and the relative signal intensities are listed in the figure, corresponding to their respective colors in the spectra.

3. RESULTS AND DISCUSSION

3.1. Selective Suppression of ^{17}O Bulk Water Signal. For the fully hydrated DMPC lipid bilayer (∼50% by weight), it was calculated to have about 40 water molecules per lipid, most of them in the bulk aqueous environment, i.e., between the lipid headgroups of opposing lipid bilayers. Thus, the ^{17}O signals are dominated by the bulk water that is highly mobile, resulting in a smaller residual quadrupolar coupling (RQC)[16,24] than the typical applied radio-frequency (RF) amplitude.[17,27] On the contrary, for those water molecules directly interacting with the lipid headgroups, especially those buried deep in this environment next to the fatty acyl carbonyl oxygens, they would retain a large quadrupolar coupling that is much greater than the RF amplitude. Consequently, these sites with different magnitudes for the quadrupolar couplings respond to the RF pulses differently. As indicated in Figure S2, the central transition of the bound ^{17}O water nutates 3

https://doi.org/10.1021/jacs.2c02145
J. Am. Chem. Soc. 2022, 144, 7881−7888

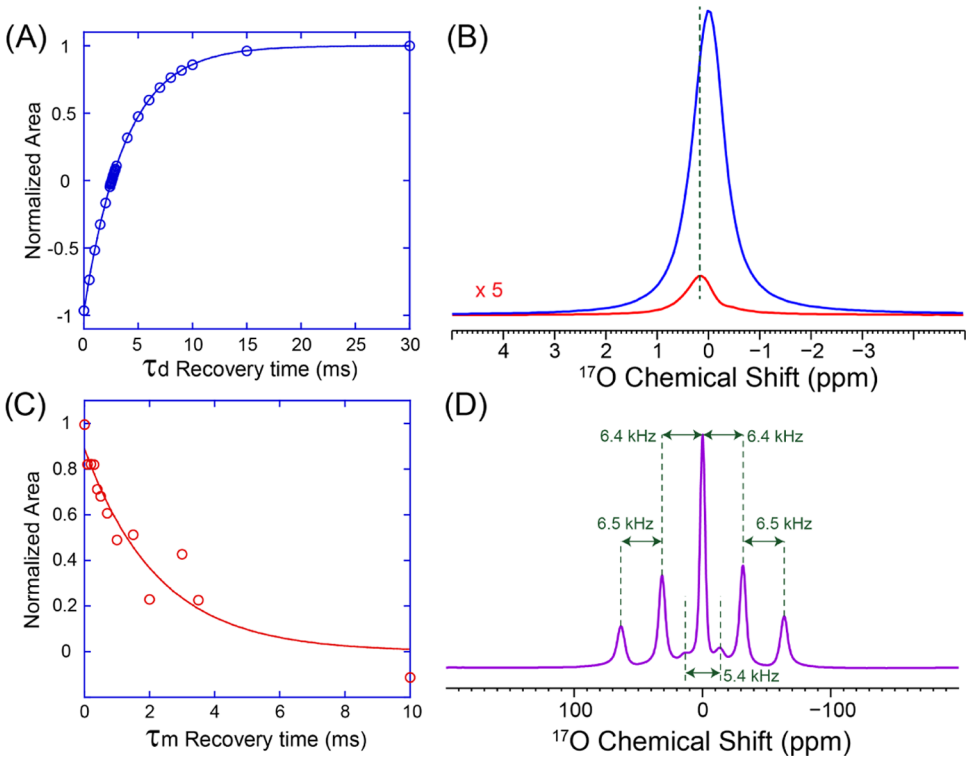

Figure 3. (A) Plot of ^{17}O bulk water signals of the hydrated DMPC bilayer as a function of τ_d; (B) ^{17}O spectra taken with different τ_d (red: 2.6 ms; blue: 30.0 ms); (C) plot of the red signal in (B) as a function of τ_m (τ_d was fixed to 2.6 ms); and (D) ^{17}O spectrum of the mechanically aligned hydrated DMPC bilayer.

times faster than the "bulk" water, so that the "bulk" water signals can be easily singled out by choosing $\theta = 60°$, where any bound water signals would simply become null. Alternatively, such bound water signals can be maximized with $\theta = 30°$, a result of the quadrupolar coupling. Due to the low population of these water molecules compared to "bulk" water, they become observable only when the dominant "bulk" water resonance is greatly suppressed. Figure S3 shows the theoretical suppression factor as a function of flip angle and indicates that the optimal central transition signal with a better suppression of the bulk water takes place with $\theta < 30°$. As shown in Figure 2B, the "bulk" water signals having a linewidth of 0.67 ppm at the half-height can be suppressed by a factor of ~500 when $n = 3$ and $\theta = 22.5°$, in contrast to just about a factor of 3 suppression in the traditional single-pulse experiments ($n = 0$ and $\theta = 22.5°$).

3.2. Dynamics of the Membrane Interfacial Water. Bulk water, as illustrated in Figure 1, whose chemical shift is set to 0 ppm, is located in the aqueous interlamellar environment. These bulk water molecules dominate the water populations compared to the lipid interfacial water and were assumed to be as dynamic as the water molecules in pure water.[34] When the 180°-pulse in Figure 2A is applied along with $\tau_m = 0$ and $\theta = 90°$, the "bulk" water is initially inverted and then recovered as a function of the delay τ_d. This inversion recovery trajectory is governed by the spin-lattice relaxation time (T_1) of the "bulk" water. As shown in Figure 3A, the ^{17}O T_1 for the "bulk" water in the DMPC bilayer was only 3.77 ± 0.01 ms, much shorter than that of the free water (8.52 ms as in Figure S4), indicating that, with ~50% hydration in our sample, there exists no "free" water as defined by "pure" water. These observations suggest a different picture: the motion of the bulk water is influenced by fast exchange (much faster than millisecond timescale) with the interfacial water molecules that are transiently and weakly interacting with the lipid choline group. In other words, the bulk water is in fast exchange with the water molecules in the lipid headgroup outer layer (as defined in Figure 1), where the motional freedom is significantly reduced.

Figure 3B shows the spectra with $\tau_d = 30.0$ ms (blue) and 2.6 ms (red). The former represents the delay where the bulk water signal is fully recovered, while the latter corresponds to the delay where the zero-crossing for the "bulk" water is taking place. Strikingly, the ^{17}O chemical shift from 2.6 ms (red) is 0.17 ppm downfield from that for 30.0 ms (blue), indicating that a small portion of the water molecules resides in a slightly different chemical environment than the dominant "bulk" water. By setting $\tau_d = 2.6$ ms to minimize the dominant "bulk" water signal and varying τ_m, we can monitor this small water signal, whose decay is determined by its specific T_1. As shown in Figure 3C, the fitting yields a T_1 value of 2.26 ± 0.38 ms, implying that there exists a small portion of water whose chemical environment and motional restriction are clearly different from that of the "bulk" water.

Although the chemical shift difference is only 0.17 ppm (~30 Hz in the SCH magnet), it undoubtedly implies that these water molecules are confined in a chemical environment having limited exchange with bulk water on a millisecond timescale, and consequently, they appear as bound on the NMR timescale. This observation might be consistent with the MD results showing anomalous anisotropic diffusion dynamics of hydration water in the lipid interface.[35] Therefore, these water molecules are defined as confined water, as illustrated in the mid-layer in Figure 1. Since there were ~40 water molecules per lipid in our fully hydrated DMPC lipid sample, we determined that 2−3 water molecules were confined per lipid by considering that their signal intensity is about 16 times

https://doi.org/10.1021/jacs.2c02145
J. Am. Chem. Soc. 2022, 144, 7881−7888

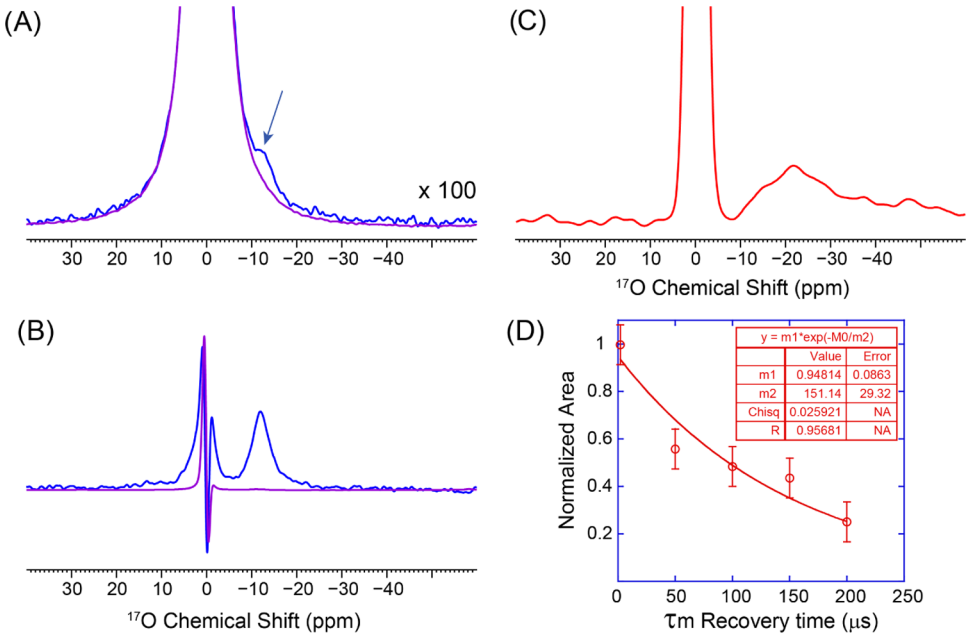

Figure 4. (A) ^{17}O spectra of the hydrated DMPC sample obtained on the SCH (35.2 T) magnet using $\theta = 22.5°$ (blue) and 60° (purple) and $n = 1$ without the 180°-pulse; (B) ^{17}O spectra of the hydrated DMPC sample as in (A) but with $n = 3$ and $\tau_d = 2.6$ ms after the 180°-pulse; (C) ^{17}O spectrum of the hydrated DMPC sample recorded on the 800 MHz NMR spectrometer under similar conditions as in (B); and (D) plot of the signal integrated from the region of −10 to −30 ppm in (B) as a function of τ_m.

less than the bulk water signal, according to the slices from the inversion recovery curve, as shown in Figure 3B. Having a T_1 value slightly shorter than bulk water as well as a small RQC (vide infra) suggests that these confined water molecules are still mobile within this confined space. We thus speculate that there exists a "pocket" in the phosphate area, which is large enough to accommodate 2−3 mobile water molecules that are somewhat isolated from the bulk water by the choline group and its waters of hydration. The most plausible "pocket" location is believed to be encapsulated between the phosphate and choline groups, having a unique environment in that the phosphate group is negatively charged and the choline group is positively charged. In fact, Chen et al. employed PS-VSFG spectroscopy[36] to investigate the phospholipid/water interface and found that the interfacial water molecules have a preferred orientation (with the water dipole oriented toward the phospholipid tails) imposed by the membrane dipole potential. Further study by Mondal et al.[7] using HD-VSFG spectroscopy reported that the interfacial water orientation in the diacylphosphatidylcholine bilayer had opposite orientations for hydrogen bonding with phosphate and choline (the positive water dipole facing the phosphate and the negative water dipole facing the choline). These VSFG studies clearly suggest the important impact that the zwitterionic phospholipid headgroup exerts on the interfacial water structure, and this long-range effect of electric field allows for the creation of a specific space that affects several water molecules, as postulated here from our NMR observation. The confined water that is stable on the millisecond timescale may structurally affect the lipid headgroup orientation and dynamics and may be of importance for membrane protein insertion or enzymatic reactivity by providing a relatively stable hydration environment, as shown in the thermodynamic study of interfacial water molecules,[37] which indicated that the surface heterogeneity of proteins may significantly increase the free-energy of the interfacial water compared to a smooth surface.

We further performed the ^{17}O measurements on an oriented sample with a similar hydration level as in the MAS sample. Figure 3D shows the ^{17}O spectrum of the mechanically aligned hydrated DMPC bilayer. Obviously, there exists a well-resolved and dominant pentad pattern with ∼6.4 kHz RQC, similar to the observation in magnetically aligned lipid nanodiscs,[27] as well as two small peaks at ∼5.4 kHz apart. These latter signals are believed to be the two inner satellite transitions stemming from ∼2.7 kHz RQC, while their outer satellite transitions (5.4 kHz) are buried under the dominant pentad pattern. The distinct chemical shift and dynamics of this small quadrupolar coupling agree with the MAS data discussed above, again confirming the existence of a small population of water that is motionally restricted. While this confined water species is not exchanging fast with "bulk" water on the NMR timescale, it still has dynamics to significantly scale the large ^{17}O quadrupolar coupling.

3.3. NMR Observation of the Membrane-Bound Interfacial Water. Figure 4A shows the ^{17}O spectra of the hydrated DMPC bilayer using different flip-angles in the pulse sequence, as shown in Figure 2A. The blue spectrum was obtained using $\theta = 22.5°$, generating the water signal at 0 ppm that is so dominant that only a small shoulder, as indicated by an arrow, could be noticed after 100-fold enlargement. When $\theta = 60°$, the small signal disappears as in the purple spectrum because the 60° flip angle will have a 180°-nutation effect on any central transition that has a large quadrupolar coupling, making its signal null. This observation confirms that the small signal at ∼−12 ppm is an ^{17}O signal stemming from water molecules that exhibit a large quadrupolar coupling. To better identify this signal, we used a seven-pulse sequence ($n = 3$) to further suppress the "bulk" water signal. Figure 4B shows the spectrum with $n = 3$ and $\tau_d = 2.6$ ms, such that the dominant signals are zero-crossing the z-axis, thereby generating

https://doi.org/10.1021/jacs.2c02145
J. Am. Chem. Soc. 2022, 144, 7881−7888

additional suppression. Clearly, the peak at −11.7 ppm with a linewidth of 4.5 ppm at half-height is well separated from the remaining bulk water signal (cf. the blue spectrum). Again, when $\theta = 60°$, this peak disappeared as in the purple spectrum. Therefore, it is confirmed that there exists bound water in the hydrated DMPC bilayer that we have been able to observe and isolate in our spectra. Since there is a unique environment per lipid for such a water molecule, any additional water molecules that would be bound would reflect a different environment and a different resonant frequency. Because a single resonance is observed, there is a single water molecule bound in this environment per lipid.

To evaluate the quadrupolar coupling and dynamics of this bound water species, we performed similar experiments on the 800 MHz instrument, about half of the field strength of the SCH magnet (1.5 GHz). As shown in Figure 4C, the ^{17}O signal at ∼−20 ppm becomes much broader and appears to have the feature of second-order quadrupolar line-broadening compared to the spectrum obtained in the SCH magnet. It is estimated that its quadrupolar coupling is on the order of MHz, significantly larger than the ^{17}O RQCs observed from magnetically aligned hydrated nanodiscs[27] as well as from the mobile water in our work on mechanically aligned lipid bilayers (cf. Figure 3D). Figure 4D shows the plot of the normalized area (from −10 to −30 ppm) as a function of τ_m. The fitting generated a T_1 value of 151 ± 29 μs, an order of magnitude shorter than that of the mobile waters. Such a substantial quadrupolar coupling and a large high-field chemical shift imply that these water molecules have strong and stable hydrogen bonding, suggesting hydrogen bonds with the fatty acyl chain ester linkages to the glycerol moiety of the lipid headgroup, as illustrated in the inner layer in Figure 1. This single extra-stable bound water is biologically, functionally, and structurally significant.

Lipid bilayers are self-assembled from lipids in an aqueous environment driven in large part by the hydrophobic effect through the formation, stability, and integrity of the hydrophobic fatty acyl chains. However, this may also be facilitated by the bound waters that may form bridges between different lipid molecules through strong hydrogen bonds with the carbonyl groups of neighboring lipids. Recent work[38] combining experimental sum-frequency generation (SFG) spectroscopy and ab initio molecular dynamics simulation also suggested the potential role of the lipid carbonyl group in stabilizing the water hydrogen-bond network. While there are proteinaceous transporters that span cell membranes and transport solutes as well as water into and out of cells, some solute and some water permeation through the lipid bilayer does occur and the stable bound water at the boundary between the hydrophobic acyl chain and hydrophilic lipid headgroup is likely to partake in this biological process.

4. CONCLUSIONS

NMR is a powerful tool for dynamic studies of biomolecules; however, standard NMR methodology is not applicable for the direct probing of interfacial water due to the extreme population difference between bulk and interfacial water. Combining ultra-high-field (1.5 GHz) spectroscopy and the selective ^{17}O solid-state NMR spectroscopy of ^{17}O-enriched water presented here has resulted in the unique observation of three distinct ^{17}O NMR resonances of water, including the "bulk" water resonance (0 ppm) that is in rapid exchange with the waters interacting with the choline in the headgroup region of hydrated DMPC lipid bilayers. In addition, there exist at least two unique types (confined and bound) of lipid hydration sites. Specifically, several water molecules denoted as "confined water" that is chemically and dynamically different from the bulk water shifted downfield by ∼0.17 ppm that showed a slightly shorter T_1 relaxation time. A third water species appears to be a single "bound water" that has severely restricted motion and a distinct chemical shift (∼12 ppm upfield) as well as an order magnitude shorter T_1 relaxation time. These latter two sites represent the most stable sites for water in the headgroup region. The existence of multiple states of water molecules in lipid bilayers had previously not been directly observed by NMR spectroscopy, as it had been proposed that the water molecules in hydrated lipid bilayers undergo very fast exchange with the bulk water (on the order of nano- and femtoseconds).[15,21,22] Our NMR results clearly show several different water states in DMPC bilayers that provide direct evidence that the water molecules reside in specific and different chemical environments, and they only experience fast exchange between the bulk aqueous environment and the aqueous environment around the choline headgroup. It is noteworthy that about 10 "bound" water molecules per lipid as characterized by ^{2}H NMR[19] are in fast exchange with the interbilayer water and thus are different from the multiple states of water molecules that we report here. In fact, the bulk water includes all water molecules between the lipid headgroups of opposing lipid bilayers and is in fast exchange with the water molecules in the lipid headgroup outer layer, i.e., the choline layer, as shown in Figure 1. Therefore, the number of water molecules in the choline layer could be characterized using the fast exchange model as in the ^{2}H NMR[19] with the mechanically oriented DMPC bilayer, where the ^{17}O residual quadrupolar coupling should depend on the water content in the lipids.

The selective ^{17}O NMR spectroscopy developed for this study can efficiently suppress the large mobile ^{17}O bulk water signals while allowing for the detection of individual water molecules in an extensively hydrated lipid bilayer environment. It is anticipated that this method can be easily extended to the studies of other interfacial water environments associated with other biomacromolecules, such as proteins, carbohydrates, and nucleic acids, where the bulk aqueous environment also hindered previous studies from being able to detect the bound water because of challenging physiological sample conditions,[39−41] providing an opportunity to characterize water dynamics on the millisecond or a slower timescale in biological systems. This study demonstrated unique capabilities of ^{17}O NMR spectroscopy at very high magnetic fields, where the ^{17}O linewidths became relatively narrow. Similar applications to other biological systems with ^{23}Na NMR spectroscopy may also be possible. Furthermore, the observed millisecond timescale of water dynamics will certainly motivate the refinement of molecular dynamic simulations for these extra-long timescales.

■ ASSOCIATED CONTENT

Supporting Information

The Supporting Information is available free of charge at https://pubs.acs.org/doi/10.1021/jacs.2c02145.

Pulse sequence design; discussions on differentiating ^{17}O signals by the size of the quadrupolar couplings and

https://doi.org/10.1021/jacs.2c02145
J. Am. Chem. Soc. 2022, 144, 7881−7888

optimizing selectivity; ^{17}O T_1 fitting for the pure water (PDF)

AUTHOR INFORMATION

Corresponding Authors

Timothy A. Cross − *National High Magnetic Field Laboratory, Tallahassee, Florida 32310, United States; Department of Chemistry and Biochemistry, Florida State University, Tallahassee, Florida 32301, United States;* orcid.org/0000-0002-9413-0505; Email: cross@magnet.fsu.edu

Riqiang Fu − *National High Magnetic Field Laboratory, Tallahassee, Florida 32310, United States;* orcid.org/0000-0003-0075-0410; Email: rfu@magnet.fsu.edu

Authors

Rongfu Zhang − *National High Magnetic Field Laboratory, Tallahassee, Florida 32310, United States; Department of Chemistry and Biochemistry, Florida State University, Tallahassee, Florida 32301, United States*

Xinhua Peng − *CAS Key Laboratory of Microscale Magnetic Resonance and Department of Modern Physics, University of Science and Technology of China, Hefei 230026, China*

Complete contact information is available at: https://pubs.acs.org/10.1021/jacs.2c02145

Notes

The authors declare no competing financial interest.

ACKNOWLEDGMENTS

All NMR experiments were carried out at the National High Magnetic Field Laboratory (NHMFL) supported by the NSF Cooperative Agreement No. DMR-1644779 and the State of Florida. Sample preparation and R.Z. were supported by NIH Grant GM122698.

REFERENCES

(1) Rothschild, L. J.; Mancinelli, R. L. Life in extreme environments. *Nature* **2001**, *409*, 1092−1101.

(2) Escribá, P. V.; Nicolson, G. L. Membrane structure and function: Relevance of lipid and protein structures in cellular physiology, pathology and therapy. *Biochim. Biophys. Acta* **2014**, *1838*, 1449−1450.

(3) Hummer, G.; Tokmakoff, A. Preface: Special Topic on Biological Water. *J. Chem. Phys.* **2014**, *141*, No. 22D101.

(4) Higuchi, Y.; Asano, Y.; Kuwahara, T.; Hishida, M. Rotational Dynamics of Water at the Phospholipid Bilayer Depending on the Head Groups Studied by Molecular Dynamics Simulations. *Langmuir* **2021**, *37*, 5329−5338.

(5) Watanabe, N.; Suga, K.; Umakoshi, H. Functional Hydration Behavior: Interrelation between Hydration and Molecular Properties at Lipid Membrane Interfaces. *J. Chem.* **2019**, *2019*, No. 4867327.

(6) Laage, D.; Elsaesser, T.; Hynes, J. T. Water Dynamics in the Hydration Shells of Biomolecules. *Chem. Rev.* **2017**, *117*, 10694−10725.

(7) Mondal, J. A.; Nihonyanagi, S.; Yamaguchi, S.; Tahara, T. Three distinct water structures at a zwitterionic lipid/water interface revealed by heterodyne-detected vibrational sum frequency generation. *J. Am. Chem. Soc.* **2012**, *134*, 7842−7850.

(8) Yamada, T.; Takahashi, N.; Tominaga, T.; Takata, S. I.; Seto, H. Dynamical Behavior of Hydration Water Molecules between Phospholipid Membranes. *J. Phys. Chem. B* **2017**, *121*, 8322−8329.

(9) Tielrooij, K. J.; Paparo, D.; Piatkowski, L.; Bakker, H. J.; Bonn, M. Dielectric relaxation dynamics of water in model membranes probed by terahertz spectroscopy. *Biophys. J.* **2009**, *97*, 2484−2492.

(10) Koch, M. H. J.; Vachette, P.; Svergun, D. I. Small-angle scattering: A view on the properties, structures and structural changes of biological macromolecules in solution. *Q. Rev. Biophys.* **2003**, *36*, 147−227.

(11) Nagle, J. F.; Tristram-Nagle, S. Structure of lipid bilayers. *Biochim. Biophys. Acta* **2000**, *1469*, 159−195.

(12) Wong, P. T. T.; Mantsch, H. H. High-presure infrared spectroscopic evidence of water binding sites in 1,2-diacyl phospholipids. *Chem. Phys. Lipids* **1988**, *46*, 213−224.

(13) Chiou, J. S.; Krishna, P. R.; Kamaya, H.; Ueda, I. Alcohols dehydrate lipid membranes: an infrared study on hydrogen bonding. *Biochim. Biophys. Acta* **1992**, *1110*, 225−233.

(14) Calero, C.; Franzese, G. Membranes with different hydration levels: The interface between bound and unbound hydration water. *J. Mol. Liq.* **2019**, *273*, 488−496.

(15) Srivastava, A.; Malik, S.; Debnath, A. Heterogeneity in structure and dynamics of water near bilayers using TIP3P and TIP4P/2005 water models. *Chem. Phys.* **2019**, *525*, No. 110396.

(16) Shen, H.; Wu, Z.; Zou, X. Interfacial Water Structure at Zwitterionic Membrane/Water Interface: The Importance of Interactions between Water and Lipid Carbonyl Groups. *ACS Omega* **2020**, *5*, 18080−18090.

(17) Paulino, J.; Yi, M.; Hung, I.; Gan, Z.; Wang, X.; Chekmenev, E. Y.; Zhou, H. X.; Cross, T. A. Functional Stability of Water Wire-Carbonyl Interactions in an Ion Channel. *Proc. Natl. Acad. Sci. U.S.A.* **2020**, *117*, 11908−11915.

(18) Volke, F.; Eisenblaetter, S.; Galle, J.; Klose, G. Dynamic properties of water at phosphatidylcholine lipid bilayer surfaces as seen by deuterium and pulsed field gradient proton NMR. *Chem. Phys. Lipids* **1994**, *70*, 121−131.

(19) Faure, C.; Bonakdar, L.; Dufourc, E. J. Determination of DMPC hydration in the L_α and $L_{\beta'}$ phases by ^2H solid state NMR of D_2O. *FEBS Lett.* **1997**, *405*, 263−266.

(20) Roy, S.; Covert, P. A.; Fitzgerald, W. R.; Hore, D. K. Biomolecular structure at solid-liquid interfaces as revealed by nonlinear optical spectroscopy. *Chem. Rev.* **2014**, *114*, 8388−8415.

(21) Mondal, S.; Mukherjee, S.; Bagchi, B. Origin of diverse time scales in the protein hydration layer solvation dynamics: A simulation study. *J. Chem. Phys.* **2017**, *147*, No. 154901.

(22) Tros, M.; Zheng, L.; Hunger, J.; Bonn, M.; Bonn, D.; Smits, G. J.; Woutersen, S. Picosecond orientational dynamics of water in living cells. *Nat. Commun.* **2017**, *8*, No. 904.

(23) Disalvo, E. A.; Pinto, O. A.; Martini, M. F.; Bouchet, A. M.; Hollmann, A.; Frías, M. A. Functional role of water in membranes updated: A tribute to Träuble. *Biochim. Biophys. Acta* **2015**, *1848*, 1552−1562.

(24) Disalvo, A.; Frias, M. The Role of Water in the Responsive Properties in Lipid Interphase of Biomimetic Systems. In *Liposomes − Advances and Perspectives*; Catala, A., Ed.; IntechOpen, 2019.

(25) Ball, P. Water as an active constituent in cell biology. *Chem. Rev.* **2008**, *108*, 74−108.

(26) Adhikari, A.; Park, W. W.; Kwon, O. H. Hydrogen-Bond Dynamics and Energetics of Biological Water. *ChemPlusChem* **2020**, *85*, 2657−2665.

(27) Ravula, T.; Sahoo, B. R.; Dai, X.; Ramamoorthy, A. Natural-abundance ^{17}O NMR spectroscopy of magnetically aligned lipid nanodiscs. *Chem. Commun.* **2020**, *56*, 9998−10001.

(28) Gan, Z.; Hung, I.; Wang, X.; Paulino, J.; Wu, G.; Litvak, I. M.; Gor'kov, P.; Brey, W. W.; Lendi, P.; Schiano, J. L.; Bird, M. D.; Dixin, I. R.; Toth, J.; Boebinger, G. S.; Cross, T. A. NMR spectroscopy up to 35.2 T using a series-connected hybrid magnet. *J. Magn. Reson.* **2017**, *284*, 125−136.

(29) Keeler, E. G.; Michaelis, V. K.; Wilson, C. B.; Hung, I.; Wang, X. L.; Gan, Z.; Griffin, R. G. High-Resolution ^{17}O NMR Spectroscopy of Structural Water. *J. Phys. Chem. B* **2019**, *123*, 3061−3067.

(30) Piatkowski, L.; de Heij, J.; Bakker, H. J. Probing the distribution of water molecules hydrating lipid membranes with ultrafast förster vibrational energy transfer. *J. Phys. Chem. B* **2013**, *117*, 1367−1377.

(31) Tristram-Nagle, S.; Nagle, J. F. Lipid bilayers: Thermodynamics, structure, fluctuations, and interactions. *Chem. Phys. Lipids* **2004**, *127*, 3−14.
(32) Kentgens, A. P. M.; Lemmens, J. J. M.; Geurts, F. M. M.; Veeman, W. S. Two-Dimensional Solid-State Nutation NMR of Half-Integer Quadrupolar Nuclei. *J. Magn. Reson.* **1987**, *71*, 62−74.
(33) Veeman, W. S. Quadrupole Nutation NMR in Solids. *Z. Naturforsch.* **1992**, *47*, 353−360.
(34) Blicharska, B.; Florkowski, Z.; Hennel, J. W.; Held, G.; Noack, F. Investigation of protein hydration by proton spin relaxation time measurements. *Biochim. Biophys. Acta* **1970**, *207*, 381−389.
(35) von Hansen, Y.; Gekle, S.; Netz, R. R. Anomalous anisotropic diffusion dynamics of hydration water at lipid membranes. *Phys. Rev. Lett.* **2013**, *111*, No. 118103.
(36) Chen, X.; Hua, W.; Huang, Z.; Allen, H. C. Interfacial water structure associated with phospholipid membranes studied by phase-sensitive vibrational sum frequency generation spectroscopy. *J. Am. Chem. Soc.* **2010**, *132*, 11336−11342.
(37) Mittal, J.; Hummer, G. Interfacial thermodynamics of confined water near molecularly rough surfaces. *Faraday Discuss.* **2010**, *146*, 341−352.
(38) Ohto, T.; Backus, E. H. G.; Hsieh, C.-S.; Sulpizi, M.; Bonn, M.; Nagata, Y. Lipid Carbonyl Groups Terminate the Hydrogen Bond Network of Membrane-Bound Water. *J. Phys. Chem. Lett.* **2015**, *6*, 4499−4503.
(39) Shweta, H.; Sen, S. Dynamics of water and ions around DNA: What is so special about them? *J. Biosci.* **2018**, *43*, 499−518.
(40) Persson, F.; Söderhjelm, P.; Halle, B. How proteins modify water dynamics. *J. Chem. Phys.* **2018**, *148*, No. 215103.
(41) Chong, S. H.; Ham, S. Anomalous Dynamics of Water Confined in Protein-Protein and Protein-DNA Interfaces. *J. Phys. Chem. Lett.* **2016**, *7*, 3967−3972.

https://doi.org/10.1021/jacs.2c02145
J. Am. Chem. Soc. 2022, 144, 7881−7888